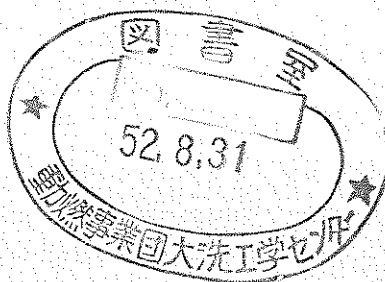


| 技術資料コード | |
|-------------------------------------|------------|
| 開示区分 | レポートNo. |
| S | N951 76-14 |
| この資料は 図書室保存資料です 閲覧には技術資料閲覧票が必要です | |
| 動力炉・核燃料開発事業団大洗工学センター技術管理室 | |

Sodium Flow Test for Dummy Core Fuel Subassemblies
of Prototype Fast Breeder Reactor MONJU

(on Pressure Loss Increase of MONJU
Dummy Core Fuel Subassemblies)



| 区分変更 | |
|---------|------------------|
| 変更後資料番号 | == |
| 決裁年月日 | 平成 13 年 7 月 31 日 |

December, 1976

本資料の全部または一部を複写・複製・転載する場合は、下記にお問い合わせください。

〒319-1184 茨城県那珂郡東海村大字村松4番地49
核燃料サイクル開発機構
技術展開部 技術協力課

Inquiries about copyright and reproduction should be addressed to:
Technical Cooperation Section,
Technology Management Division,
Japan Nuclear Cycle Development Institute
4-49 Muramatsu, Tokai-mura, Naka-gun, Ibaraki, 319-1184
Japan

© 核燃料サイクル開発機構 (Japan Nuclear Cycle Development Institute)



PNC TSN951 76-14

NOT FOR PUBLICATION

PNC TSN951 76-14

December, 1976

Sodium Flow Test for Dummy Core Fuel Subassemblies
of Prototype Fast Breeder Reactor MONJU
on Pressure Loss Increase of MONJU
Dummy Core Fuel Subassemblies

Tetsuro Fujimoto*, Kazujiro Sato*,
and June Takahashi*.

A b s t r a c t

The 4,800-hour flow test for MONJU dummy core fuel subassemblies was carried out at sodium flow rate of 19.5 ~ 20.2 kg/sec. subassembly, sodium temperature of 600°C, and oxygen impurities in sodium of 2 ~ 2.5 ppm which are about the same condition as that for MONJU core fuel subassemblies.

The result of this test showed that the pressure loss of dummy core fuel subassemblies increased up to 11% in 3,000 hours and became constant after that.

The integrity of the dummy subassemblies is planned to be investi-

This is the translation of the Report, No. SN941 76-47, issued in May, 1976.

* Fluid Dynamics Section Sodium Engineering Division, Oarai Engineering Center, PNC.

gated by disassembling them and making a material examination.

On the other hand, the pressure loss increase for these subassemblies was estimated at 5.4% in case of water flow test which was carried out before and after sodium test.

The cause of this difference should be investigated hereafter.

C O N T E N T S

| | Page |
|---|------|
| 1. Introduction ----- | 1 |
| 2. Test Loop ----- | 2 |
| 2-1. Test Loop and Measuring Instruments ----- | 2 |
| 2-2. Dummy Core Fuel Subassemblies ----- | 4 |
| 3. Test Method ----- | 6 |
| 3-1. Sodium Flow Endurance Test ----- | 6 |
| 3-2. Loading and Unloading of Subassemblies ----- | 9 |
| 3-3. Cleaning of Subassemblies ----- | 10 |
| 4. Test Results and Review ----- | 12 |
| 4-1. Results of Sodium Flow Test ----- | 13 |
| 4-2. Results of Hydrodynamic Test ----- | 14 |
| 4-3. Comparison between Sodium Flow Test and Water Flow Test ----- | 15 |
| 4-4. Studies on Pressure Loss Increase of Various Sections of Fuel Subassembly ----- | 19 |
| 4-5. Pressure Loss Increase and Corrosion Rate ----- | 23 |
| 5. Conclusion ----- | 26 |
| 6. Acknowledgements ----- | 27 |
| 7. References ----- | 28 |

1. Introduction

The development of fuel subassemblies for the Proto-type fast breeder reactor "MONJU" has been carried out by four domestic makers and by PNC at its Plutonium Fuel Development Facility, Tokai Works.

The Sodium Flow Test Facility exposed the second trial-made dummy fuel subassemblies to a series of experiments in order to examine pressure loss increase phenomenon of fuel subassemblies. The experiments involved hydrodynamic tests before and after a sodium flow endurance test of the dummy subassemblies.

The phenomenon of pressure loss increase of fuel subassemblies was discovered ⁽¹⁾ when the sodium flow endurance tests of the dummy subassemblies for the core of the experimental fast breeder reactor "JOYO" were carried out. As its phenomenon has influence on the flow distribution in the core if it occurs in nuclear reactor. Its quantitative determination has been desired.

However, it is very difficult to determine it for lack of long-term stability and accuracy of measuring instruments, and hydrodynamic tests by water were performed before and after the sodium flow endurance test for the purpose of obtaining backup data.

During this experiment, two wire-spacer type subassemblies (made by Hitachi and NFI) out of those 2nd trial-made core fuel subassemblies having approximately equivalent pressure loss were loaded into the test section in the sodium flow test loop, and tested under the same condition of MONJU as much as possible for about 4,800 hours from May 27 to December 16, 1975.

2. Test Loop

2-1. Test Loop and Measuring Instruments

The test loop used for this experiment was PNC's Sodium Flow Test Loop, and the experiment was performed by loading the dummy core fuel subassemblies into the test section of the loop. As the description of the test loop was introduced by various reports already, no further description is given here. As to the type of measuring instruments and their performance accuracy are given as follows: (Refer to Fig. 2-1 "Schematic Diagram of Sodium Flow Test Loop" and Fig. 2-2 "MONJU T/S of Sodium Flow Test Loop".)

(1) Sodium Flowmeter

There are four flow meters in Sodium Flow Test Loop, one is orifice type the others are electromagnetic type. But out of them, only one electromagnetic type (permanent magnetic) was actually calibrated for precision accuracy so that its output signals could be used as the basis for the adjustment of data. This type of flowmeters had been calibrated to the actual sodium flow at the Sodium Component Test Facility of PNC, and its performance error is below $\pm 1.7\%$ in the total flow region.

(2) Thermometers (C.A. Thermocouples)

C.A. thermocouples of class 0.75 were employed for measuring sodium temperatures. The measured temperature error was thought to be below $\pm 5^{\circ}\text{C}$. Although these thermocouples measured sodium temperatures by means of thermocouple wells, there was no particular problem experienced since measurement was made under normal

constant conditions.

(3) Pressure Gauges

For the measurement of pressure loss, three pressure gauges were installed in the test section. The specifications of these pressure gauges are as shown by Table 2-1. This type of pressure gauge was of zero-shift in its long time use. Its shift rate seemed to be affected by room temperatures, sodium temperatures and sodium exposure hours. Because of this, it is necessary to apply calibration to each of them in each case of measurement in order to obtain data of higher accuracy. In the present experiment, the pressure gauges were calibrated in the covergas atmosphere within the range of 0.0 ~ 1.5 kg/cm. before and after the endurance test, and also zero-point checkup was performed in each case of flow test.

As this zero-point checkup was made in the presence of sodium in the test section, it was difficult to attain any absolute calibration due to fluctuation of sodium level. Because of this, the zero-point shift rate was assessed relatively by making relative calibration of performance among the gauges.

As we used the values after assessment of this zero-point shift rate for the pressure loss data, its error was below 0.5%. The results of the absolute calibration in the state of sodium drain before and after the test showed hardly any change in the gradient in the first approximate expression and only zero-point shift existed. Since this zero-shift rate approximately matched

with the result of the relative calibration at the time of the final sodium flow test, it was considered there was no problem in the calibration method of pressure gauges.

2-2. Dummy Core Fuel Subassemblies

The dummy core fuel subassemblies used for the present experiment were those two second trial-made subassemblies out of those five which were made based on the third design of MONJU. These two subassemblies were of the wire type core fuel subassemblies made by NFI and by Hitachi Limited. These two subassemblies are quite identical both in material and construction to the actual MONJU's core fuel subassemblies except in the following four points only: ① They are provided with static pressure taps for hydrodynamic test (it is, however, blinded by weld at the time of sodium flow endurance test); ② their spherical seats as well as the diameter and the length of the terminal end of the entrance nozzle are changed in order to match them to the test section; ③ the pad positions of the wrapper tubes are unified; and ④ the fuel pellets are simulated by SUS. Fig. 2-3 and 2-4 represent their construction, and Table 2-2 shows their specifications. These subassemblies, after delivery, were first exposed to dimensional measuring tests at the Fuel & Material Assessment Section, PNC's Tokai Works, and then to hydrodynamic tests at the Hydrodynamic Test Section of PNC's Oarai Engineering Center. Thereafter, they were alcohol washed and dried and were loaded into the test section.

The hydrodynamic test was performed for the purpose of measuring the pressure losses at various sections of the subassemblies and thus to obtain the basic data to be reflected to the core design and to be used for the assessment of pressure loss increase phenomenon. The details of this hydrodynamic test are to be reported separately.

3. Test Method

3-1. Sodium Flow Endurance Test

The sodium flow endurance test was conducted at the sodium flow loop (refer to Fig. 2-1 and 2-2) by loading into the test section as shown in Fig. 2-5, two types of second trial-made subassemblies, of which one was M2CWG made by NFI, and the other was M2CWH made by Hitachi Limited, and also five dummy subassemblies (one of which was provided with grooves for protection of static pressure taps).

The sodium flow endurance test was performed under the following conditions and care in order to satisfy as much as possible the requirements of the actual core fuel system of MONJU: ① Sodium plug temperature below 150°C ; ② sodium flow rate at 20.2 kg/sec/per subassembly; ③ sodium temperature at 600°C (395°C at the inlet and 588°C at the outlet of the real reactor core, and its integral average temperature at 514°C); ④ absolutely no sodium draining unless required by reason of safety so that no subassemblies be exposed to cover gas during the endurance test. The methods taken to satisfy these requirements are given as follows:

a) Sodium Purity Control

For keeping the higher purity of loop's sodium, sodium purification operation was undertaken seven times prior to the commencement of the experiment. The impurities trapped in the cold trap were drained each time into the cold trap drain tank. After loading the fuel subassemblies into the test section, sodium was charged into the test loop from the dump-tank. In this case, the

sodium temperature was maintained as low as possible at 216°C . As the result, it was possible to maintain the plug and unplug temperatures immediately after sodium charge and during the 36 hours of sodium purification and temperature raising operation on such a highly favorable level at 136°C for the former and at 163°C for the latter. For the entire experimental period, the minimum temperature of the cold trap mesh was maintained at 143°C except in an abnormal time. As the result, since the plug temperatures were $130^{\circ}\text{C} \sim 140^{\circ}\text{C}$ and unplug temperatures $145^{\circ}\text{C} \sim 155^{\circ}\text{C}$, it might as well be said that, from the solubility curves of Eichelberger, oxygen concentration of about 2 ppm could be maintained. The reason for the temporal failure in holding this cold trap condition was that because of the occurrence of plugging of the cold trap after about 3,800 hours from the initiation of the test, regeneration work had to be performed requiring about five whole days and nights during which period, the loop's sodium could not be purified by cold trap. Because of this, the plug temperature of the loop's sodium rose to 147°C and the unplug temperature up to 170°C . Fig. 3-1 shows the sodium purification situation during the test period.

b) Sodium Flow Rate

The sodium flow rate was set to match MONJU's rated flow rate at 20.2 kg/sec ($1.5 \text{ m}^3/\text{min}$ at 600°C) at the outset of the experiment. But due to the subsequent pressure loss increase phenomenon of fuel subassemblies, the flow rate gradually declined. However, because of the designed test section pressure of 5 kg/cm^2 and the

pressure gauge in the range of $-1 \sim 5 \text{ kg/cm}^2$, it was impossible to maintain the rated flow rate under such a pressure condition. And thus the pump's revolution was maintained at a certain set revolution number, as the result, the pressure loss of fuel subassemblies was kept nearly constant. The sodium flow endurance test was carried out by this method, and the test measuring was performed by temporally increasing the flow rate.

(c) Sodium Temperature

Although the sodium temperature under normal condition was $600^\circ\text{C} \pm 5^\circ\text{C}$, it was lowered to $510^\circ\text{C} \sim 540^\circ\text{C}$ at the time of the calibration of the pressure gauges. This was done in each flow test at the rate of about 1 ~ 2 hours/one time. In the event of power interruption by thunderbolt striking, there was a case where the sodium temperature dropped for several hours by malfunction of heaters. Fig. 3-3 shows the sodium flow rates and temperatures during the entire test period, while Table 3-1 gives the test conditions.

(d) Holding in Argon Covergas

During the test period, there was no case of fuel subassemblies being exposed to the argon covergas atmosphere. Though fuel subassemblies might have been exposed to high temperature argon covergas atmosphere (250°C) at the time of loop preheating prior to the charging of sodium and also at the time of sodium draining, there was no fear of much problem since the argon gas purity at this time was 99.99% having contained no much impurities such as

especially oxygen.

3-2. Loading and Unloading of Fuel Subassemblies

Loading of fuel subassemblies into the test section was carried out by blowing argon gas into the test section at the room temperature and sealing it with a sheet of vinyl cover so that no air would enter into the test loop. The situation after loading fuel subassemblies is as shown by Fig. 2-5. As seen from the diagram, there is a center dummy in the mid-center (newly designed and made so that it can be installed into the test section without removing the static pressure tap which is provided for a hydrodynamic test of subassemblies), and there are arranged two subassemblies and four dummies surrounding it. Thereafter, a control plate is installed in the test section and a blind flange is provided before the commencement of the test.

Unloading of subassemblies after finishing the test was performed in the following manner: Sodium was drained at 350°C . Thereafter the test section was maintained at 350°C for about three hours by pre-heater. Then the pre-heater was switched off to cool it for about 48 hours. As the result, the temperature of the test section dropped to 150°C . Then the control plate and the blind flange were removed, and then the core fuel subassemblies were extracted. The force needed for the extraction was about one ton. The weight of the subassemblies being 200 kg, a force more than five times stronger than this weight was necessary to extract them. The reason for this was that, due to short preheating time after sodium drain, sodium had not been completely drained and the residual sodium had coagulated (this was thought as

the result of temperature drop in between the subassembly and the test section), and thus, in order to shear or compress coagulated sodium, such a force was assumed to be necessary.

For extraction of subassemblies, a vinyl cover sheet was used to seal off air to prevent subassemblies from contacting air and argon gas blown into the test section all while during this extraction operation. There was a case where the residual sodium surface presented dark color, which was the color of some oxides produced as the result of reaction of sodium with a small quantity of oxygen, and which turned to gray after exposed to air.

After the extraction of the subassemblies, they were kept in a atmosphere of argon gas for cooling, and then were washed.

3-3. Cleaning of Subassemblies

Cleaning of subassemblies was performed first by using ethyl alcohol, and then by gradually adding water. For the assessment of the residual sodium inside the subassemblies, the washing liquid was sampled at each appropriate time for analysis, which was performed by a neutralization-titration method to quantify. The results are as shown in Fig. 2-6. The acid standard solution used for the analysis was 1/10 NH_4Cl , and methyl orange was used to determine its neutrality. The Hitachi made subassemblies (M2CWH) out of the two types of subassemblies retained a large quantity of residual sodium at their entrance nozzle due to insufficient sodium draining from the test section, and thus a large quantity of sodium was detected. Consequently, it was assumed as the result of the assessment of the subassemblies of NFI (M2CMG) that 65g

was the standard residual sodium quantity of MONJU's core fuel subassemblies in the case of the test loop of the present experiment.

Studies on the effects upon materials by cleaning are very scarce. But according to the report of F. Casteels et al,⁽⁷⁾ it seemed such effects were small. Nevertheless, as there would be the same depositions which might be removed from the material surface by cleaning, thus making it difficult to allow real scientific and rigorous observation of material surface conditions.

4. Test Results and Review

The present sodium flow endurance test of the newly trial made core fuel subassemblies was performed with the purpose of satisfying as much as possible the conditions of the real MONJU reactor core. As the results, the sodium purity control (oxygen concentration) was satisfactorily achieved, and approximately constant conditions had been maintained relating to temperatures and flow rates except for such unavoidable situation as data collection and power interruption. Likewise, for the unloading and extracting fuel subassemblies after finishing the experiment, and for the subsequent cleaning and hydrodynamic tests, the best methods available at the present stage were taken and followed. Therefore, it may be said that the experiment had satisfied the real MONJU reactor core conditions except that there existed no thermal flux, and thus it was thought the assessment of the pressure loss increase phenomenon which was the target of our experiment was possible. The following pages will be dedicated for the description of the results of our sodium test on the pressure loss increase phenomenon, and also our review on the results of the hydrodynamic tests undertaken at out PNC's Hydrodynamic Test Facility before and after the sodium flow test of the present core fuel subassemblies.

4-1. Results of Sodium Flow Test

The sodium flow test was carried out at the rate of once in every 500 hours approximately in order to measure and confirm the compatibility of fuel subassemblies and pressure loss variation. For the collection of pressure loss data, temperature was maintained at a constant

level ($600^{\circ}\text{C} \pm 5^{\circ}\text{C}$) and was measured with flow rate as parameter, while the test conditions were maintained constant as much as possible at all times. But as flow rate had to be dropped to zero at the time of pressure gauge calibration, there was an instance when temperature was down to nearly a 500°C level.

The accuracy of this sodium flow test was that flowmeter accuracy above $\pm 1.7\%$, pressure gauge accuracy $\pm 1.0\%$ (nominal accuracy was $\pm 0.5\%$). But it was assumed from the zero-drift rate at the time of its calibration), and temperature accuracy $\pm 0.75\%$. Consequently, the obtained pressure loss coefficient accuracy was $\pm 4.0\%$ approximately. However, since it had been confirmed that there was hardly any time lapse change of the performance of electromagnetic flowmeters, although the accuracy to flow rate absolute value was $\pm 1.7\%$, it would be all right to consider the output signal monitoring instrument accuracy of $\pm 0.1\%$ as the flow rate accuracy in the case of making assessment of time lapse change of accuracy.

Therefore the assessment accuracy of pressure loss increase phenomenon is about $\pm 2.1\%$.

The results of the sodium flow test are given in Table 4-1 and Fig. 4-1 respectively.

Table 4-1 shows the results of the sodium flow test rearranged into the form of $C_d = aRe^{-b}$ by use of a least square mean method and the results of the hydrodynamic tests performed before and after the sodium flow test. The data of pressure loss increase phenomenon at the rated Re number ($\approx 75,000$) of MONJU's core fuel subassemblies are given in Fig. 4-2, from which it is known that the increase of pressure loss of the

core fuel subassemblies stops after about 3,000 hours and thereafter it remains approximately constant.

In the evaluation of the sodium flow test accuracy, as the pressure gauges were calibrated only to the extent of $0 \text{ kg/cm}^2\text{G} \sim 1.5 \text{ kg/cm}^2\text{G}$, the accuracy of pressure gauge at the high pressure plenum (PX2-2) ($-1.0 \sim 5.0 \text{ kg/cm}^2$) in the test section was within this extent only, and for $1.5 \text{ kg/cm}^2\text{G}$ and above, a linearity was assumed. The calibration extent of this pressure gauge is restricted by the pressure resistant of mechanical sealing sections of the mechanical pumps in the loop. Besides the errors of measuring instruments, the sodium leakage from the gaps and spaces between the spherical seats of the seven fuel subassemblies and the receiving seats in the test section constitutes a factor of error. As the subassemblies are held by the hydraulic hold down force, they may apt to float causing abrupt change of pressure loss data. Fortunately, however, in the present experiment such phenomenon did not occur, and it was safe to consider only the leakage from the micro gap between the spherical seat and the receiving seat. This leak may vary due to vibration of subassemblies and also to the scratch or flaw produced in the spherical seat after their loading. In the present experiment, however, no evaluation was possible in this respect.

4-2. Results of Hydrodynamic Test

In order to determine the flow dynamic performance of the core fuel subassemblies and the variation in the sodium flow characteristics in the case of sodium flow test, a series of hydrodynamic tests of fuel subassemblies were carried out because of the advantages of this type

of test in collecting experimental data more easily. The detailed report on this hydrodynamic test is contemplated to be made in a near future. But here, we have presented in Table 4-2 (a) and (b), and Fig. 4-3 (a) and (b) the necessary data which are considered to be important in discussing the pressure loss increase phenomenon. The accuracy of hydrodynamic test data was $\pm 1\%$. But the data accuracy at the entrance nozzle section was $\pm 3\%$. The pressure loss of the shield had an added pressure losses of part of the pin bundle, entrance nozzle outlet and of the handling head because of the location of the pressure tap.

There were two types of subassemblies, one of which (M2CWG) was exposed to this hydrodynamic test after one week of sodium drain, and the other (M2CWH) after three weeks of sodium drain. Also M2CWG was again subjected to the same test after four weeks of sodium drain to confirm no resulting effect. Therefore, it was made clear that keeping them in atmosphere after cleaning had no relation with pressure loss increase phenomenon.

4-3. Comparison between Sodium Flow Test and Hydrodynamic Test

The results of both the sodium flow test and the hydrodynamic test were subjected to non-dimensional rearrangement using the values of the flow channel cross section and the hydraulic diameter obtained from the measurements of the fuel subassembly at a room temperature. As the material of the subassembly was SUS316 and its expansion coefficient was $\alpha = 18.5 \times 10^{-6} (^{\circ}\text{C})^{-1}$, in the case of the sodium flow test at 600°C , its

dimensions expanded, such as flow channel cross section by 2.23%, hydraulic diameter by 1.11% and length by 1.11%. Consequently, its flow velocity became smaller by 2.23% and its Re number by 1.11%. Because of this, the pressure loss coefficient increased by about 4.3% should indicate the real pressure loss caused by flow.

$(C_d = aRe^{-b} \rightarrow C_d = 1.045 \cdot a \cdot (\frac{1}{0.989})^{-b} \cdot Re^{-b})$ also elongated by about 1% and accordingly the sodium flow test data may show large values to match this value. Therefore, the pressure loss coefficient by the sodium flow test as shown in Table 4-1 should be enlarged 4.3% to represent the real experimental values. As previously described, the accuracy of the sodium flow test data was $\pm 4\%$ while the accuracy of the hydrodynamic test was $\pm 1\%$, and considering that the dimensional expansion rate was 1% it was known that the pressure loss coefficient immediately after sodium exposure was within the range of the error.

Then the results of the hydrodynamic test after finishing the sodium flow test and sodium flow test immediately before the sodium drain were compared. Considering the dimensional changes, the results of the sodium flow test were about 10% larger, while accuracies in both cases of sodium flow and hydrodynamic tests were unexplainable.

Here, seeking some other possible factors, they may be cited as follows:

- 1) Accuracy of sodium pressure gauges
- 2) Time lapse variation of sodium flowmeters
- 3) Effects of sodium cleaning and hydrodynamic test
- 4) Effects from the difference of test sections
- 5) Underestimation of sodium viscosity coefficient

The accuracy of pressure gauges and flowmeters is described previously.

The pressure gauges, especially the high pressure plenum pressure gauge PX2-2, were used for a long time at nearly the maximum point (5 kg/cm^2) in the range of $-1 \sim 5.0 \text{ kg/cm}^2$, and besides, they had not been calibrated in that range of pressure. While in this calibrated pressure range, the pressure sensing diaphragm showed growing fatigue with the lapse of test time (output signal grew larger). Its linearity was, however, good.

There are examples ⁽⁶⁾ to show by the flowmeters actually taken out from test loop that there is not time lapse change of performance of flowmeters. But in the case of flowmeters to be used many hours in high temperature, it is difficult to deny that no change would take place in the size and distribution of magnetic flux density by the variation of material properties and dimensions.

Then in the next, the reason for citing the effects of cleaning and hydrodynamic tests as the possible factors for the difference between the two resulting data as given above is that these effects have the possibility of causing some changes on the surface conditions of fuel subassemblies. That is, the possibilities of such phenomena as excoriation and leaching of deposited substance on the surface of metals, or deposition of some floating substances in the water. These, however, are the inevitable phenomena as long as the present form of test procedures are pursued. Because of this, we must endeavor to improve sodium test accuracy so that we are able to evaluate flow dynamic performance by the sodium test data.

The pressure of the high pressure plenum in the test section of the sodium test loop during the present sodium flow test was measured at upstream of flow streightner. Therefore, such pressure loss as occurring at the flow streightner and the pressure loss caused by the entrance nozzle of dummy subassemblies were also counted as the pressure loss of the subassemblies themselves. But due to small flow velocity, their effects were little. It is not necessarily impossible to concieve an idea of possibility that, at the time of loading subassemblies into the test section, there might occur incursion of foreign matters such as sodium oxides or chips of metal in-between the spherical seats of the subassemblies and the receiving seats of the test section to cause sodium leak to the upper section. But it is impossible with the present test section to detect and evaluate sodium leak from spherical seats. It is, therefore, necessary to make effort to eliminate any questions arising from the test section structure.

Underestimation of viscosity coefficient derives from the impurities in solid form existing in sodium⁽¹⁰⁾. But as the effect of concentration of such solid impurities becomes evident when it reaches the level of 10^4 ppm, it may be unnecessary to consider this problem in the present experiment.

We have so far reviewed the difference in the flow performance by the sodium flow test and by the hydrodynamic test conducted after the sodium flow test. There are only two conceivable factors for the reason of larger pressure loss in the case of the sodium flow test. Namely, problems of reliability of pressure gauge accuracy and effects of cleaning. Other problems do not constitute any major effects to

cause pressure loss decline or increase. The reason for doubt as to pressure gauge reliability is because calibration of pressure gauges have not been made upto the high pressure region. But assuming from the pressure gauge's linearity not fluctuating too much, it is not considered too serious. Consequently, the cleaning effect may be considered as the major cause. This judgement is based on the reports that ① although pump's overflow rate declined with the progress of time, it recovered its normal function after it was washed,^(8,9) and ② there was experienced in the CCTL = MK-II experiment that by cleaning subassemblies, there had ceased pressure loss increase.

4-4. Studies on Pressure Loss Increase Phenomena of Various Sections of Fuel Subassemblies

The following facts can be cited as the pressure loss increase phenomenon experienced in the present sodium flow test:

When tested under the conditions of Re number about 84,000 ~ 86,000, temperature at 600°C, and in-sodium oxygen concentration at 2 ~ 2.5 ppm by Eichelberger's equation, the subassembly pressure loss showed an abrupt increase at the initial stage and thereafter turned to gradual increase, and after 2,500 ~ 3,000 hours, it became approximately constant, and then subsequently remained with almost no change (refer to Fig. 3-2). (The initial abrupt pressure loss increase may be due to the rapid progress of corrosion as the result of 20% cold work of the fuel pin clad (cf. JOYO 10%). This pressure loss increase rate was about $11\% \pm 2.5\%$. This value owes to the good accuracy of pressure gauges so long as there is existing no time lapse variation in the

functional performance of pressure gauges as previously stated. This has been obtained by working an expression obtained from the sodium flow test at the point of rated Re number 75,000. Although it has been earlier referred to in respect of the difference between the results of the sodium flow test and those of the hydrodynamic test, the pressure loss increase in the comparison with the data of the hydrodynamic test was $5.4\% \pm 1\%$. The reason for this difference is not clear so far yet, and from the results of the hydrodynamic test, the time lapse variation of various sections of fuel subassemblies will be studied in qualitative pursuit of the causes of pressure loss increase. (Refer to Fig. 4-3 (a) and (b), and Table 4-2 (a) and (b)).

a) Entrance Nozzle

The pressure loss of entrance nozzles is mostly due to contraction and expansion. But the reason for the different values between M2CWH of which is about 1.6 and M2CWG of which is about 2.5 are considered due to the effect of the difference in the chambering of orifices. Also, for the reasons of pressure loss increase, even though very small, it is conceivable that the surface roughness of the orifices presents some fluctuation which helps raise pressure loss. Its ratio in proportion to the total pressure loss is not only so small, but also so small is its pressure loss variation rate that it does not necessarily constitute any cause for the pressure loss increase phenomenon of fuel subassemblies.

b) Lower Shield

The pressure loss in this area includes those pressure loss

at the outlet of entrance nozzle and at the bundle inlet. When pressure loss caused by bundle friction is assessed by use of the coefficient of bundle friction loss, the rectified values are 1.59 for M2CWG and 2.47 for M2CWH before the sodium flow test and 1.65 for M2CWG and 2.63 for M2CWH after the sodium flow test. These figures indicate pressure loss increase even at the shield itself.

c) Pin Bundle Section

The pressure loss increase at the pin bundle section is 4.9% for M2CWG and 6.4% for M2CWH. Of these data obtained by the hydrodynamic test, the pre-sodium flow test data are larger by small margin in the higher Re number region comparing with the values of $f_{Re} = 2 \times 10^4 = 0.0266$, $f_{Re} = 7.5 \times 10^4 = 0.0191$ as obtained from Blasius Eq. The reason for this is that, since the wire wound around pins affects the flow rate distribution in the subchannels and also produces secondary stream, it is difficult to sufficiently explain the flow condition by Re number which we defined. Rehme, Nonendstern, Sangster, et al. have reported their expressions using wire winding pitch, pin diameter, pin intervals, wire diameter, etc. as parameters. However, in the case of the fuel subassemblies used for the present experiment, the peripheral pins are wound by wire of different diameter and pitches from those of the central pin in order to prevent the effect of the surrounding flow (swirl flow caused by wire). Consequently, further consideration is necessary for any assessment of pressure loss by use of these expression as proposed.

Because of this, it is considered questionable to directly link surface roughness to pressure loss increase quantitatively by Cole-Brook equation and Moody's Diagram using Re number which is thought not to sufficiently represent the flow condition. However, according to the hitherto obtained test results, their cause and effect relations have been qualitatively confirmed, and therefore, when the surface roughness of these subassemblies is obtained by Cole-Brook Eq., the resulting values are $0.66 \mu\text{m}$ for M2CWG and $0.99 \mu\text{m}$ for M2CWH. The clad surface roughness before sodium exposure has been measured as about $0.8 \mu\text{m}$ (R_{max}). Consequently, it may well be said that the measured surface roughness and that of Cole-Brook's Equation do not directly link to each other. Linking of roughness variation to pressure loss increase will be discussed further after the roughness measurement to be performed after the disassembling of the subassemblies. It is also necessary to clarify the relation between the so measured roughness and fluid dynamic roughness.

Then in the next, when the ratio of friction loss of the bundle section in proportion to the entire pressure loss is sought, it is 74.8% for M2CWG and 76.0% for M2CWH in the case of pre-sodium flow test, while it is 74.8% for M2CWG and 75.4% for M2CWH in the case of post-sodium flow test. Likewise, the ratio of the bundle section for pressure loss increase is 73.6% for M2CWG and 67.1% for M2CWH. Therefore, it is clear that pressure loss increase is caused not only by the bundle section alone, but also in several other sections.

d) Upper Shield (Including Handling Head)

Assessment of friction loss of the bundle section at this zone gives the following values: $M2CWG = 1.80$ and $M2CWH = 2.36$ in the case of pre-sodium flow test, and $M2CWG = 1.89$ and $M2CWH = 2.49$ in the case of post-sodium flow test. Consequently, the pressure loss at the shield, handling head and bundle outlet is 1.51 for $M2CWG$ and 1.3 for $M2CWH$ in the case of pre-sodium flow test and 1.61 for $M2CWG$ and 1.47 for $M2CWH$ in the case of post-sodium flow test. As the result, it is known that there also exists pressure loss increase even at the shield and the handling head.

From the results of the hydrodynamic test, the total pressure loss increase rate in the case of $M2CWG$ is indicated small, due to the small pressure loss increase rate in various sections other than the bundle section. While in the case of $M2CWH$, the pressure loss increase rates are approximately the same in all sections. As to the pressure loss increase in the bundle section, it is qualitatively explainable by reason of the increase of surface roughness.

4-5. Pressure Loss Increase Phenomenon and Corrosion Rate

In the next, consideration was given to causes of surface roughness changes and its mechanism. It is well known that materials are corroded by sodium. This corrosion rate is subject to temperature, sodium purity (oxygen concentration), flow velocity (thickness of Laminar sublayer), exposure time, downstream, etc. Also by the configuration and form of test loops as well as by temperature gap, material

corrosion rate is greatly influenced. There are any corrosion products in sodium and its behavior has a correlation with corrosion mechanism. There are many reports published relating to corrosion, behavior of corrosion products (deposition and adhesion). But due to the existence of so many parameters, it is difficult to establish a generalized expression which is applicable to cases in broad range. PNC's Sodium Flow Test Facility has conducted experiments on mockup fuel subassemblies for both JOYO and MONJU, but only sodium purity (oxygen concentration) and flow velocity have changed. (JOYO and MONJU have different downstreams).

After finishing these experiments, the cladding materials were subjected to inspection. The result indicated increased material surface roughness, and the surface condition presented either corrosion or deposition of corrosion products covering the surface. It is known that this difference is due to the influence of oxygen concentration rate.

The present experiment was conducted at a low rate of in-sodium oxygen concentration maintained constantly all during the test period at 2 ~ 2.5 ppm using Eichelberger Eq. For the observation of corroded material surface, it is expected to be done after disassembly of the subassemblies. At any rate, an increase of surface roughness by mass transfer on the surface of the cladding materials can well be expected.

Here, in Fig. 4-4 presented are the results of correlation between corrosion and pressure loss. Here, as corrosion rate (R_c) is the function of ① oxygen concentration (C_{ox}), ② temperature (T), and ③ Reynolds number (Re), their effects are assumed to be indicated in the form of the following listed equation, and by inserting in it the term

of hour to define corrosion factors,

$$R_c = A \cdot C_{ox} \cdot e^{-\frac{17500}{R T}} \cdot Re^{0.8}$$

R = gas constant (1.987 cal/g mole °K)

* For activated energy, Thorley's 17500 cal/mole was used.

$$R_{cf} = \int R_c dt = \int C_{ox} \cdot e^{-\frac{17500}{R T}} \cdot Re^{0.8} dt$$

R_{cf} = corrosion factor (hr·ppm)

For the assessment of oxygen concentration, Eichelberger's expression was employed (For this corrosion factor definition, such physical property values which are considered to be more reasonable at present have been employed).

By defining the corrosion factors, it became possible to be compared with other data. And thus the data of JOYO and FFTF were also shown together. Pressure loss increase does not directly link to corrosion (also existed were the effects of cold work rate and fluid dynamic diameter). There existed some questions in the definition of corrosion factors, and not necessarily obtainable any good agreement between them. Consequently, it is thought necessary to do more efforts in accumulating data and reviewing evaluation methods.

5. Conclusion

The present sodium flow experiment of the 2nd trial-made core fuel subassemblies for "MONJU" was undertaken under the conditions of sodium temperature at 600°C, in-sodium oxygen concentration at 2.0 ~ 2.5 ppm constantly, sodium flow rate at 1.5 m³/min/one subassembly for the duration of about 4,800 hours in continuation. As the result, some useful data relating to Pressure loss increase phenomenon of fuel subassemblies have been obtained indicating that pressure loss increased about 11% at 3,000 hours, while thereafter it remained approximately constant.

Meanwhile, hydrodynamic tests were performed before and after the above mentioned sodium flow test. The results of the test showed a pressure loss increase by about 5.4%. The reason for such different values has not been made clear yet even though several studies were made. It is considered necessary to do further efforts for raising the reliability of data by improving the calibration system of sodium measuring instruments, by further studying the structure and construction of the test section as well as the effects of sodium cleaning.

As to the compatibility and integrity of fuel subassemblies, and also relating to the studies on the mechanism of pressure loss increase phenomenon by conducting material tests, these will be reported separately on other occasion after completion of the disassembly inspection.

6. Acknowledgements

The words of our thanks are hereby expressed to all persons concerned for their assistance and cooperation extended in connection with the present experimental work. Particularly, to Mr. R. Saito, Manager of Sodium Engineering Div., Dr. K. Mochizuki, Dr. K. Uematsu and Mr. K. Kamimura of PNC head office. We also owe much to the advice and supervision provided by Prof. Ishibashi of Ohita University.

7. References

- (1) Ishibashi and Himeno, "Sodium Flow Test on JOYO Mockup Core Fuel Subassemblies (2) - (6)". PNC Reports SN941 71-14, SN941 74-17, SN941 74-65, SN941 75-67, SN941 75-76.
- (2) R.L. Myers HEDL-TME 72-39. HEDL-TME 74-8.
- (3) GEAP-10394.
- (4) Ishibashi et al. "Outline of Sodium Flow Heat Transfer Test Loop" SN941 71-15.
- (5) Sasaki et al. "Sodium Flow Heat Transfer Test Loop, Modified 2" PNC Reports, SN941 74-75.
- (6) Uno et al. "Sodium Flowmeter Calibration Test" (Part 4), PNC Report SN941 75-69.
- (7) F. Casteels, M.J. Fevery - De Meyer et al. Corrosion Daciers Ferritiques et Austenitiques Dons Le Sodium Influence des Methodes de Nettoyage.
- (8) Akema et al. "In-Sodium Endurance Test of JOYO's Primary Main Circulation Pump" SN941 74-68.
- (9) Tanaka, Uno et al. "Overhauling, Washing and Installation of JOYO's Primary Main Circulation Pump Mockup-3" SN941 75-96.
- (10) Landau - Lifshitz Fluid Dynamics, Tokyo Tosho

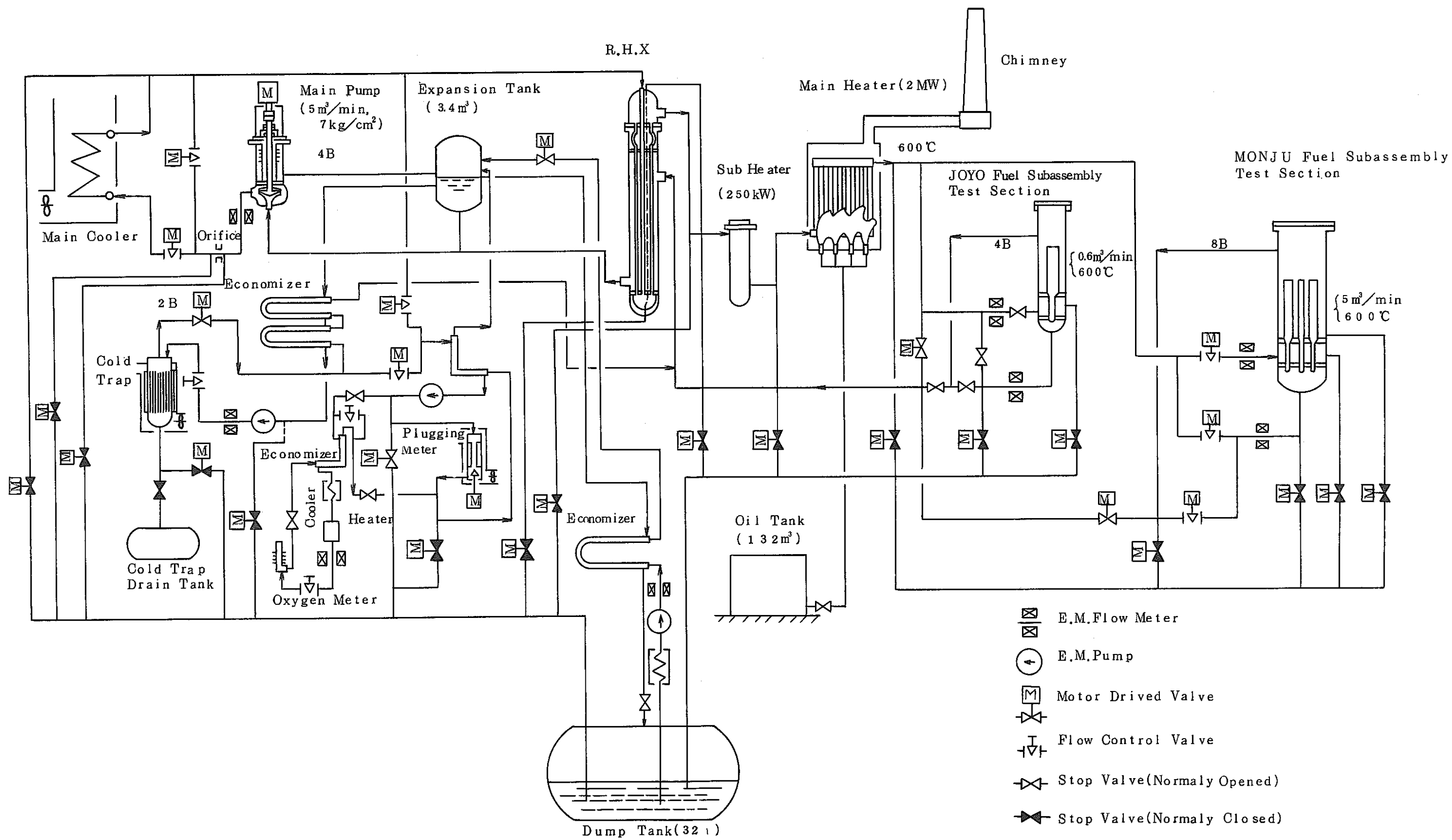


Fig.2.1 Schematic Diagram of Sodium Flow Test Loop

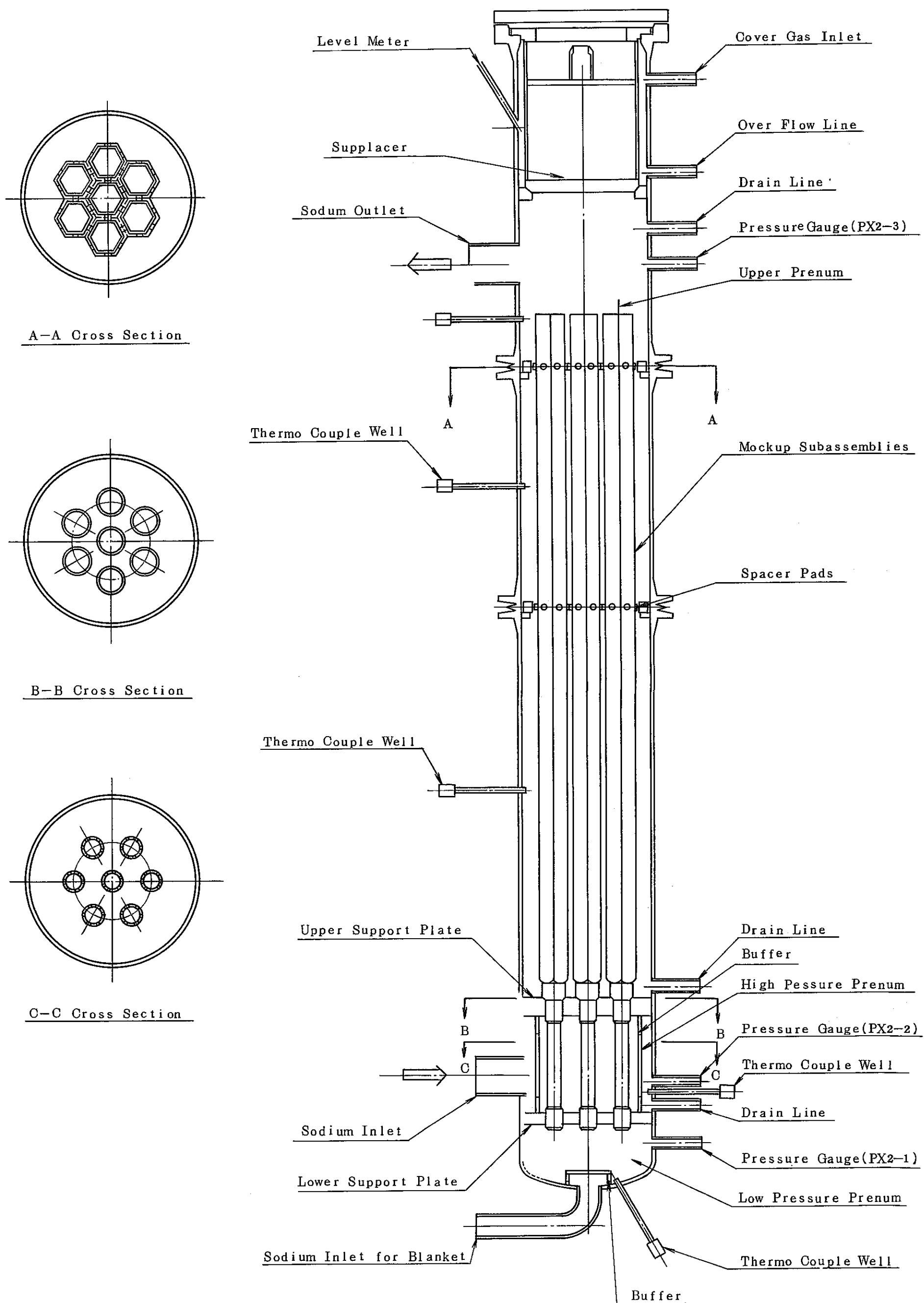


Fig 2.2 MONJU T/S of Sodium Flow Test Loop

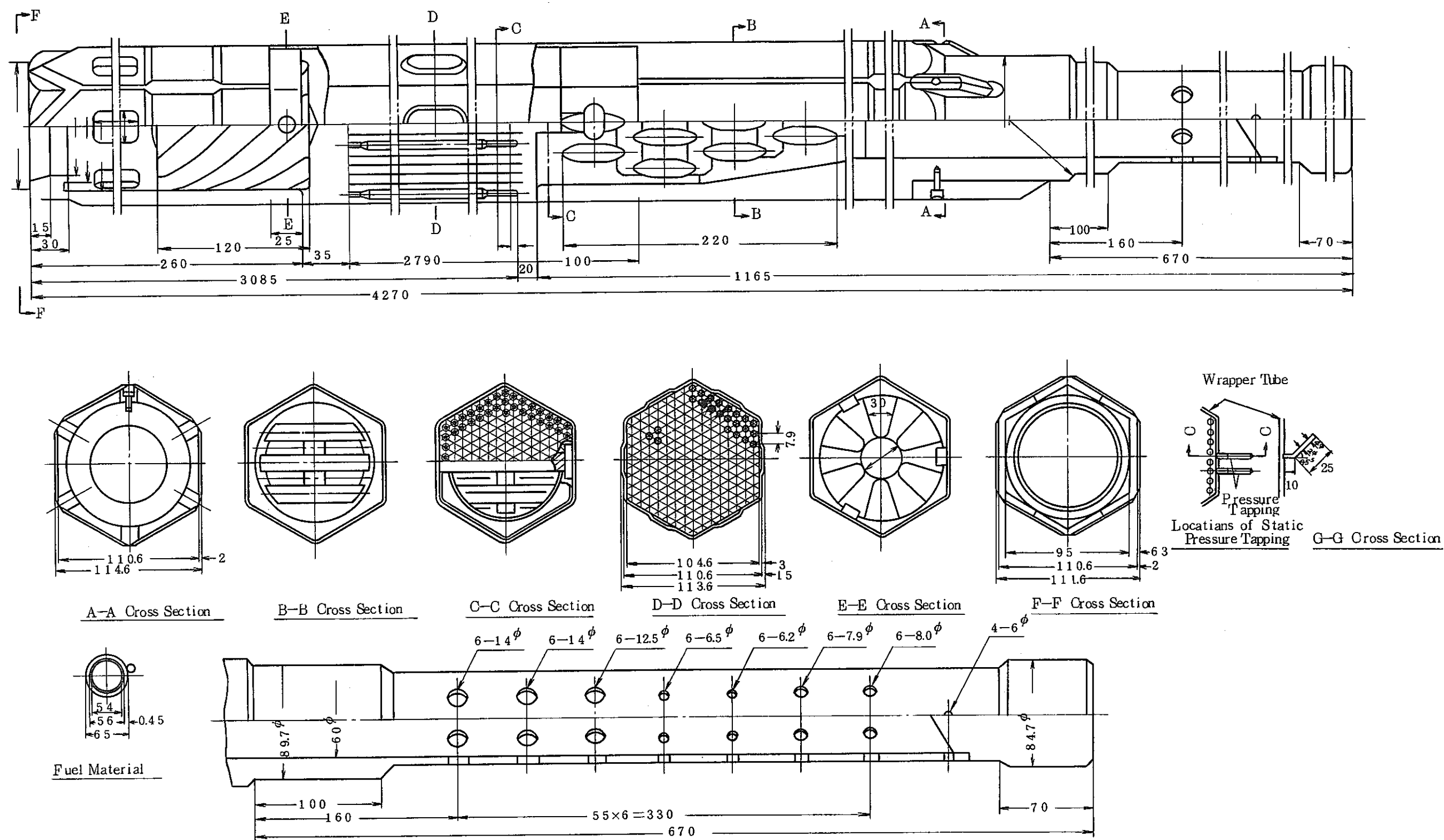


Fig 23 Core Fuel Subassembly (M2CWG)

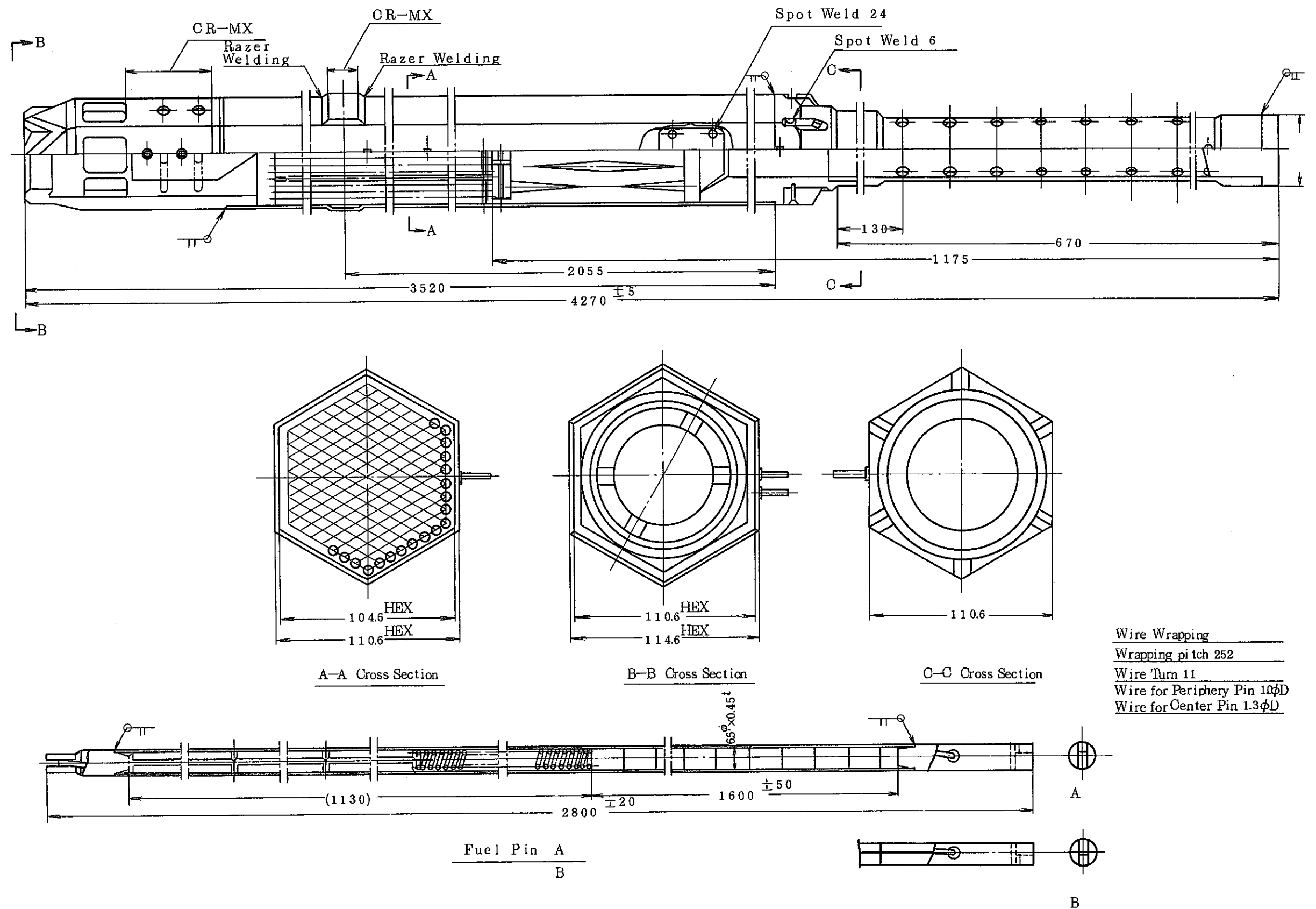


Fig24 Core Subassembly (M2CWH)

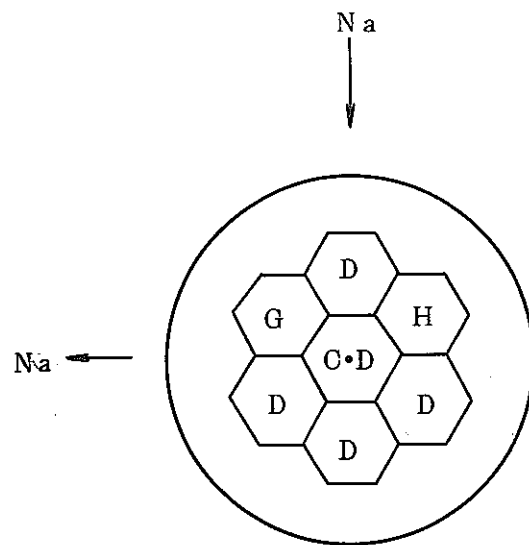
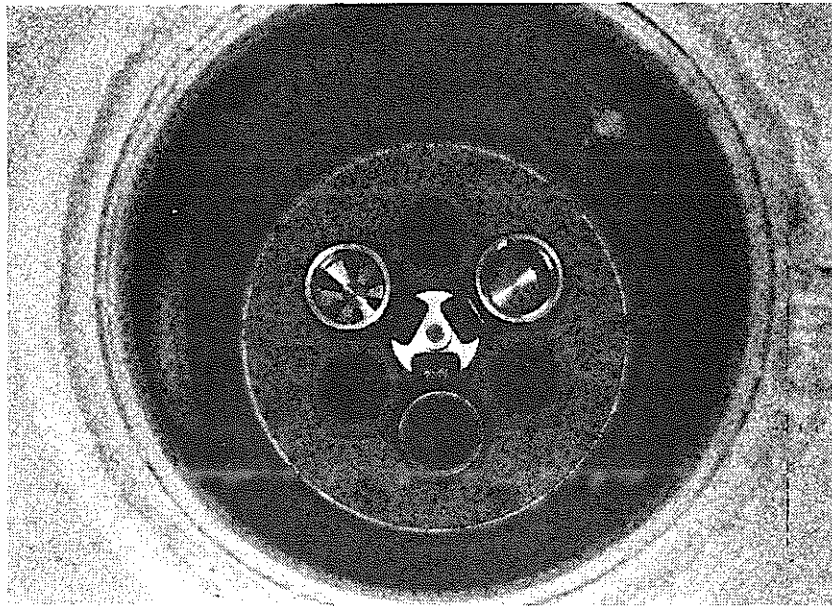


Fig.2.5 F/A Lay-out at MONJU Test Section
 (G;M2CWG H;M2CWH D;Dummy F/A
 CD; Center Dummy)

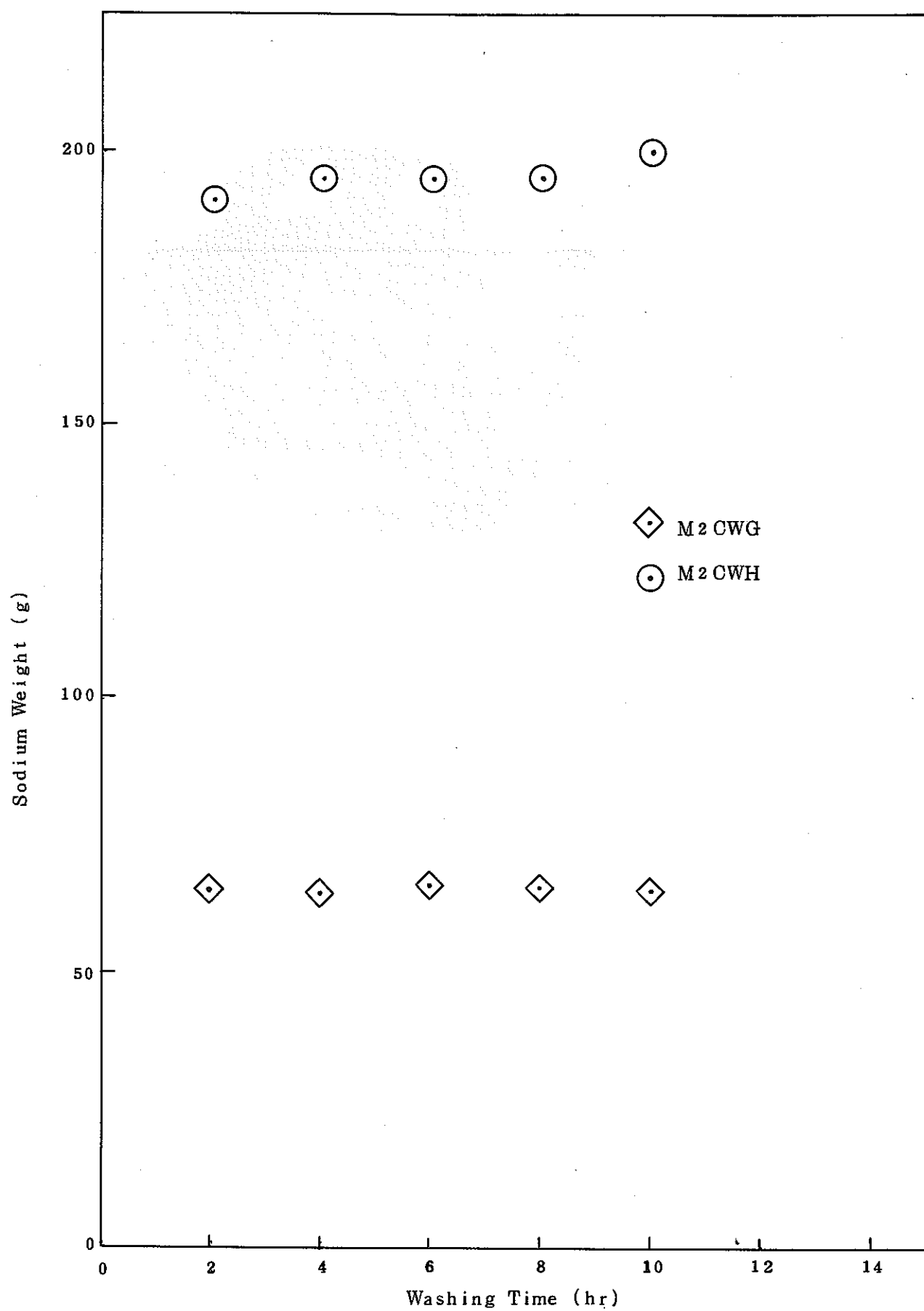


Fig 2.6 Chemical Analysis Result of F/A Washing Solution(C_2H_5OH)

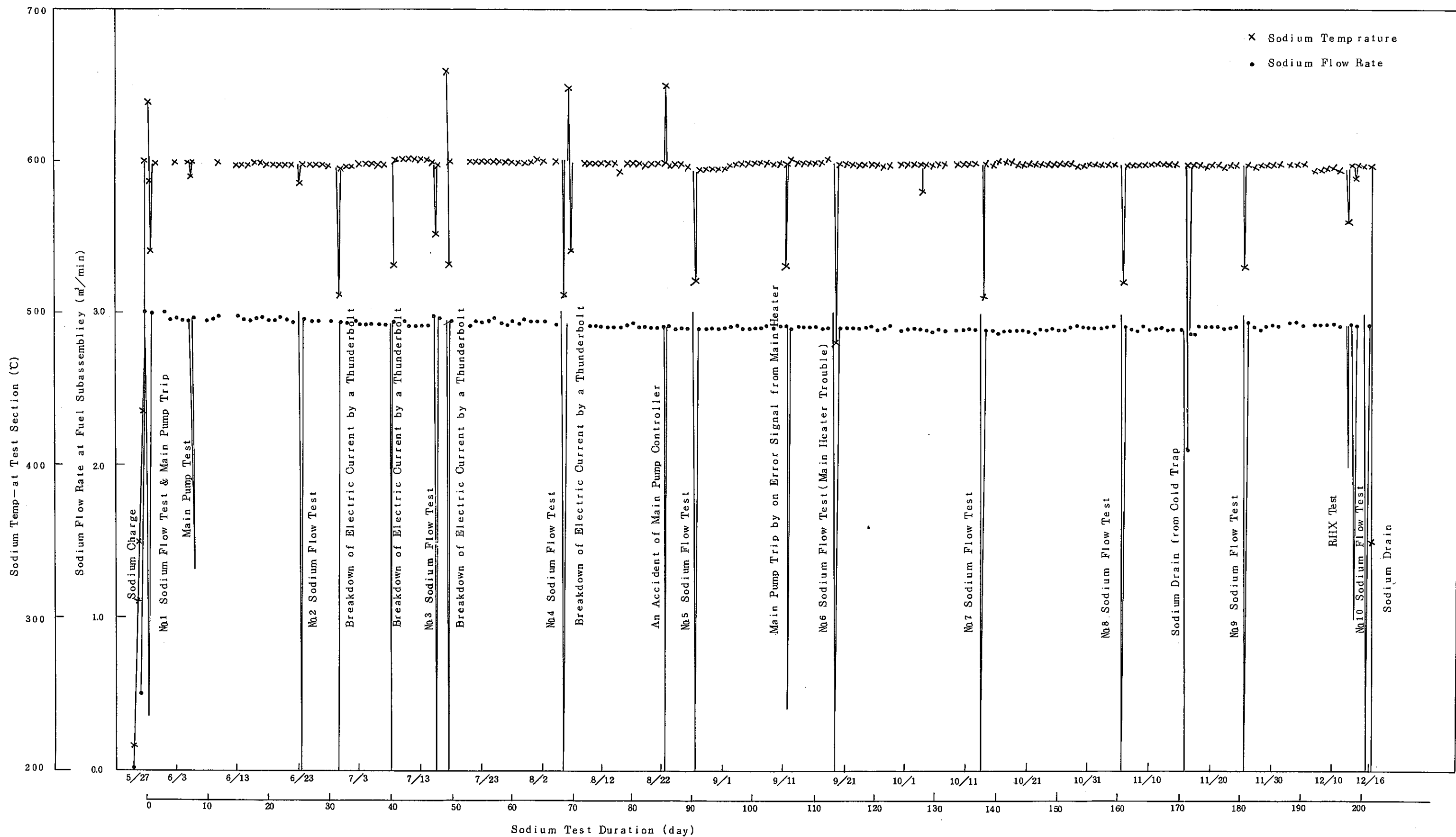


Fig.3.1 Dummy Fuel Subassemblies Endurance Test Record

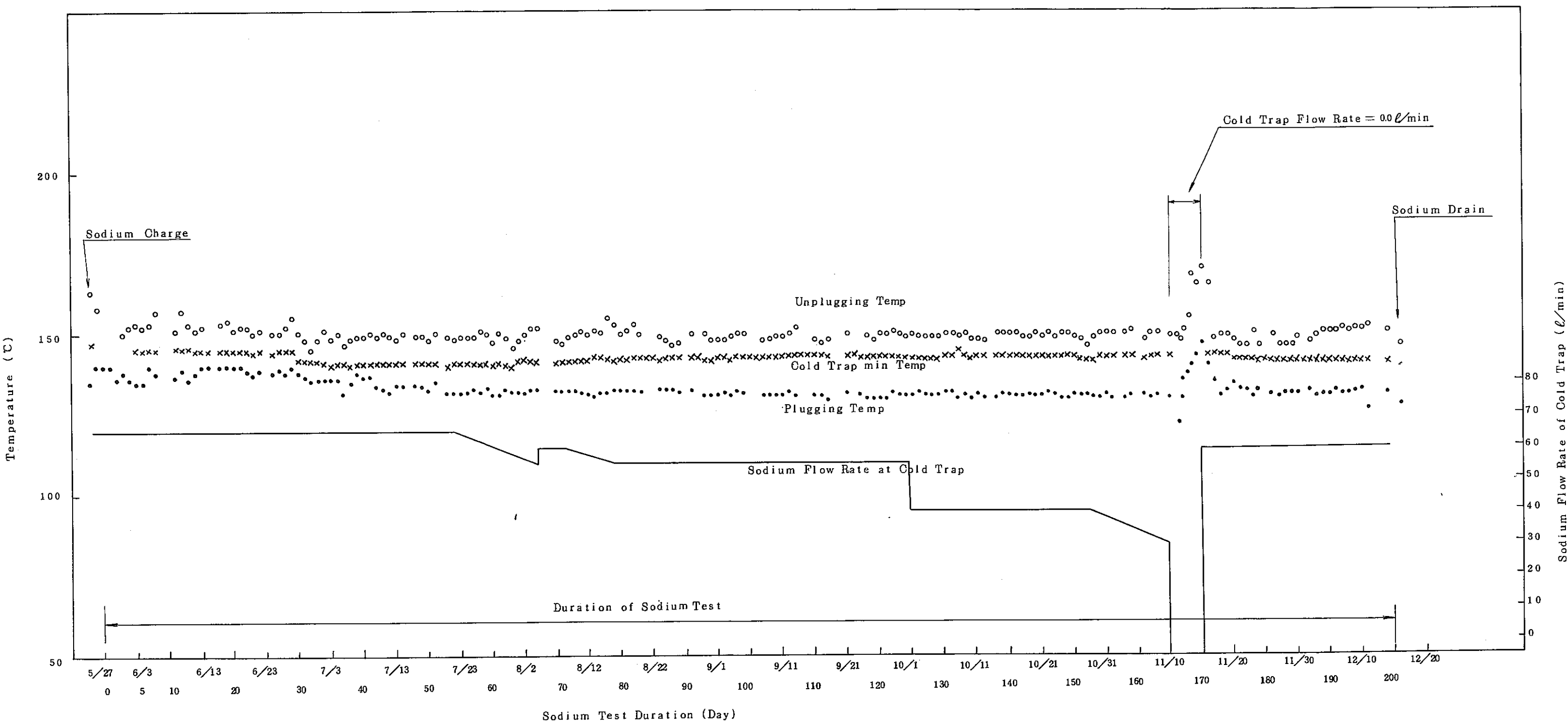


Fig 3.2 Sodium Purity Control Record of F/S Endurance Test MONJU(II)

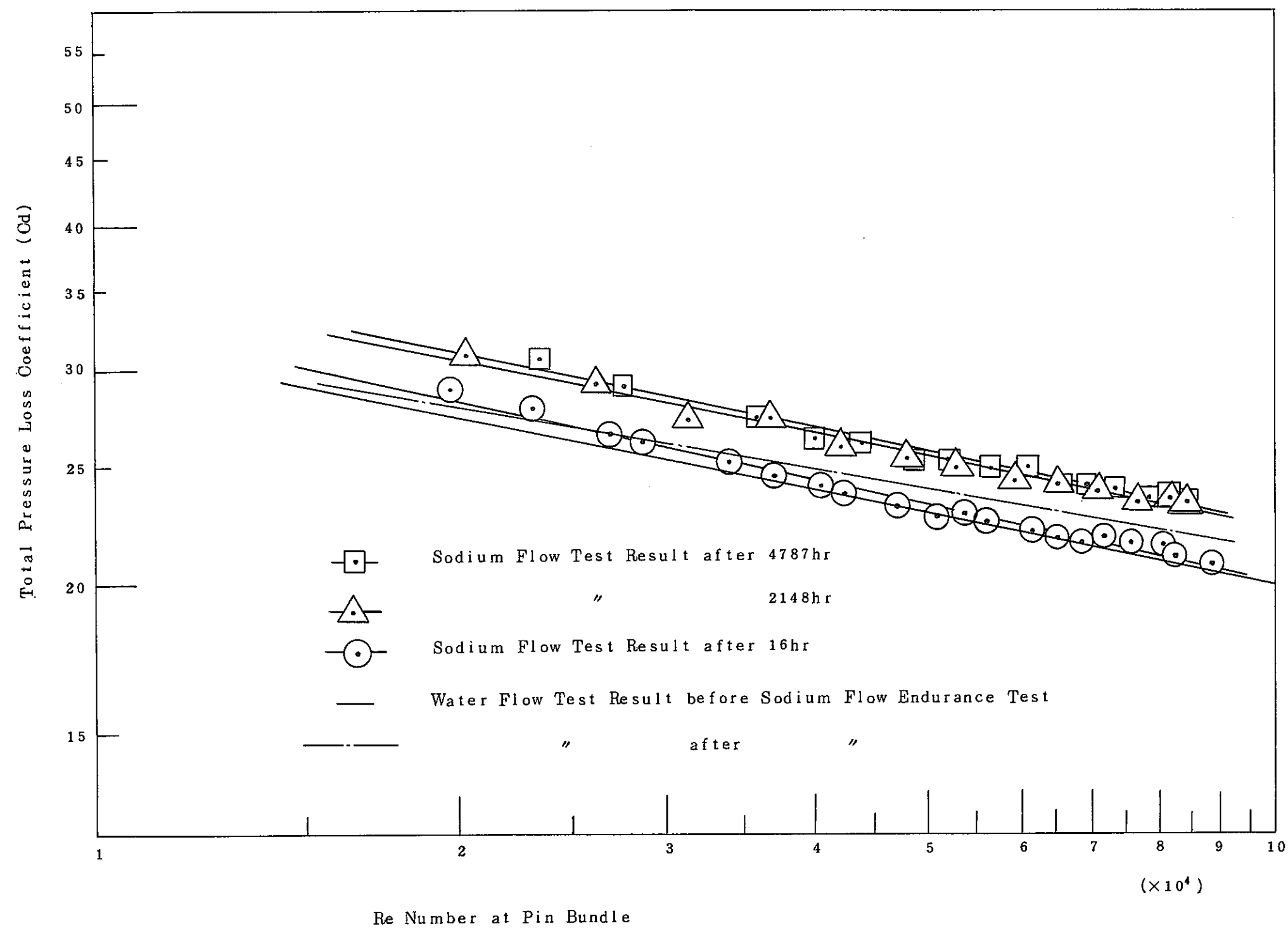


Fig 41 Sodium Flow Test Results of MONJU (II)

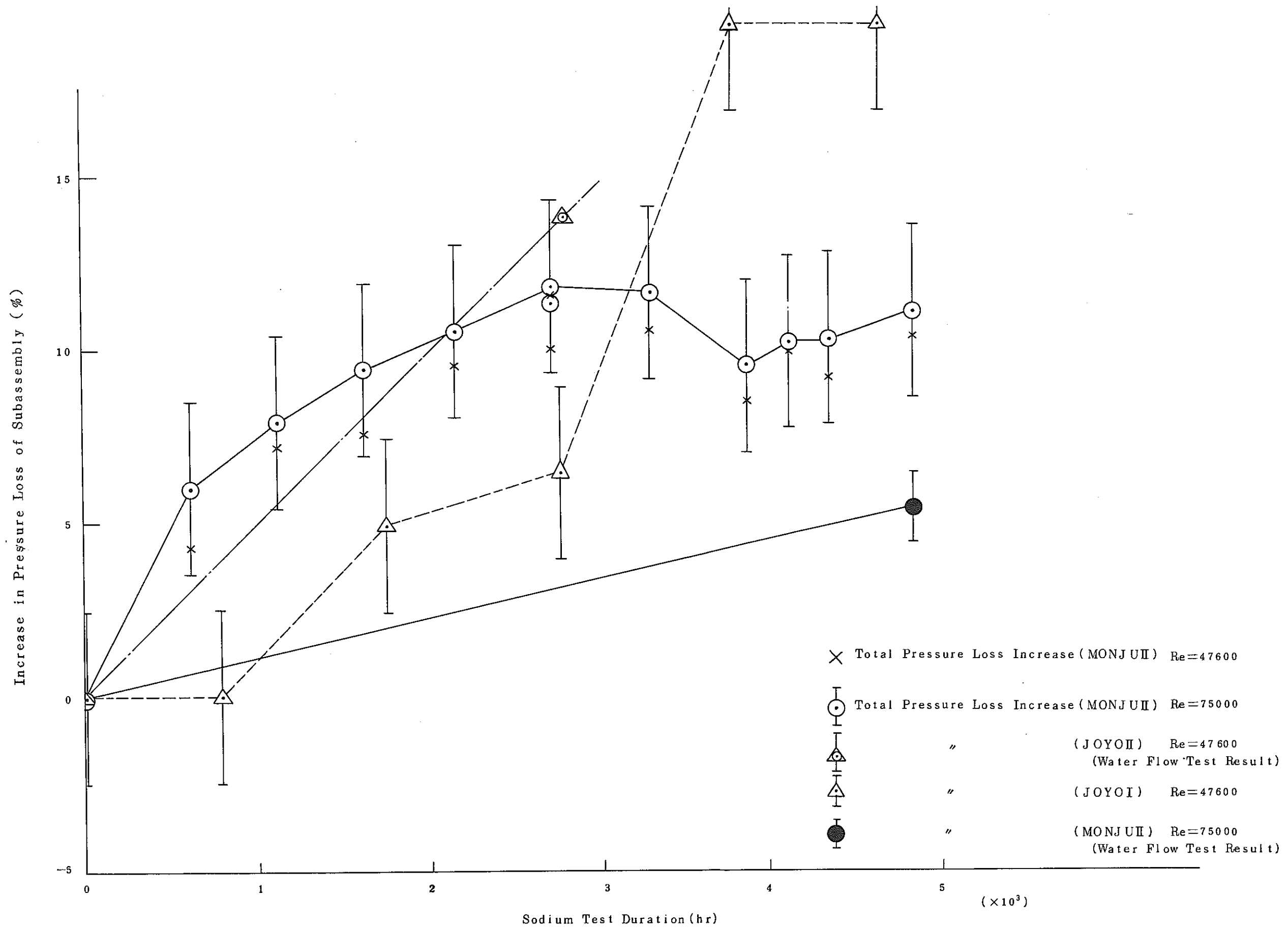


Fig 4.2 Total Pressure Loss Increase of Fuel Subassemblies at Rated Re Number

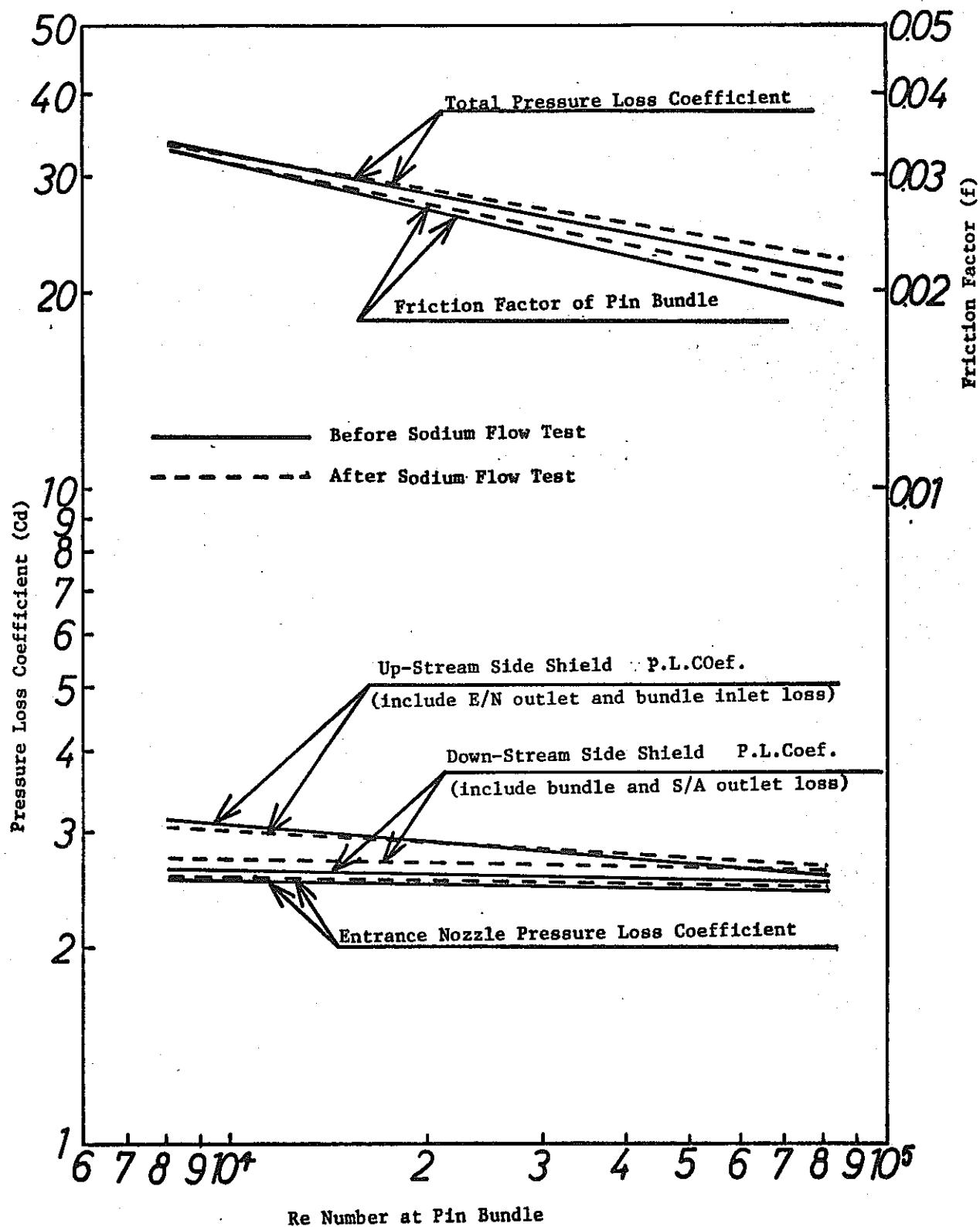


Fig.4.3.(a) Pressure Loss Coefficients and Friction Factor of M2CWG by Hydrodynamic Test

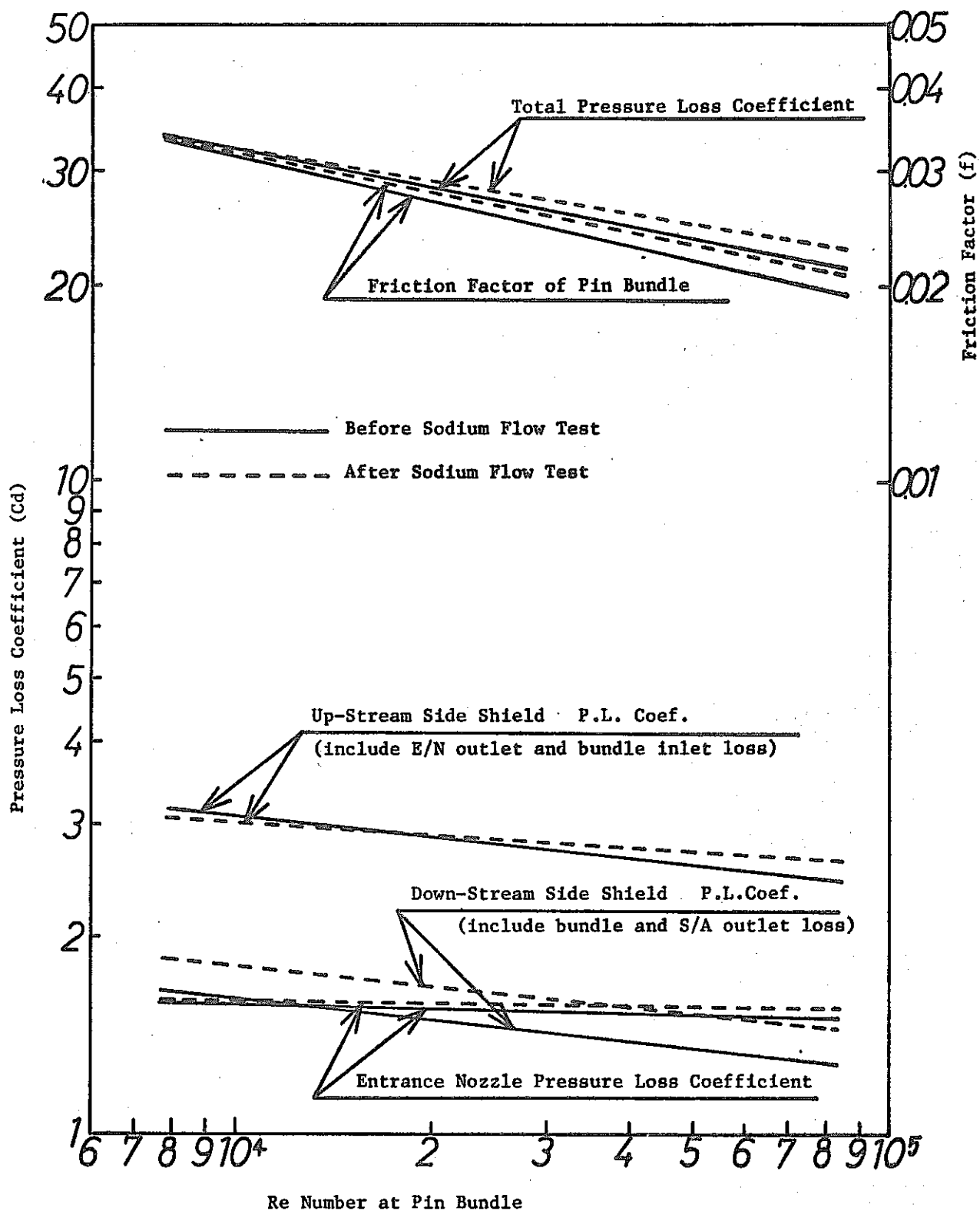


Fig.4.3(b) Pressure Loss Coefficients and Friction Factor of M2CWH by Hydrodynamic Test.

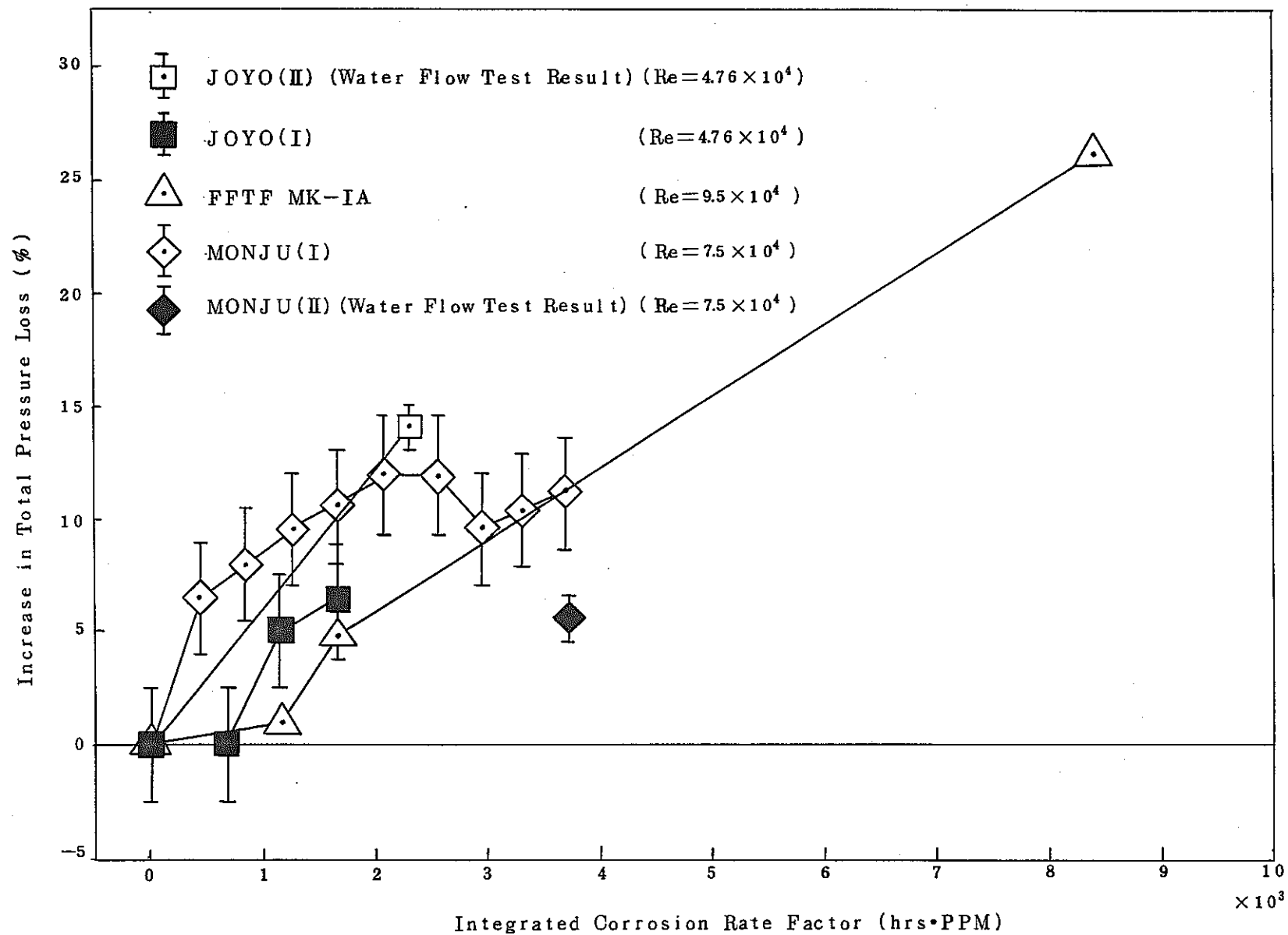


Fig 4.4 Total Pressue Loss Increase-Corrosion Rate Factor Relationship at Rated Re Number (Eichelberger Eq was used)

Table 2.1 Specifications of Sodium Pressure Gauges

| Pressure Gauges | Class | Range (kg/cm ²) | Setting Point | Type |
|--------------------|-------|--------------------------------|-------------------------|------------|
| PX 2-1 | 0.5 | -1~2 | Low Pressure Prenum | EPR-3 S(W) |
| PX 2-2 | 0.5 | -1~5 | High Pressure Prenum | EPR-3 S(W) |
| PX 2-3 | 0.5 | -1~2 | Exit | EPR-3 S(W) |

Table 2.2 Specifications of MONJU Mock-up Wire Type Fuel Subassembly

| <div>Item</div> <div>Subassembly Name</div> | Fuel Pin | | | Assembly | | Wire Spacer | | | | Hydraulic | Flow Cross Section | Entrance Nozzle Orifice |
|---|----------|--------|--------|----------|--------------------|-------------|-------|-----------|-------|-----------------|--------------------|-------------------------|
| | Dia. | Length | Number | Length | Wrapper tube scale | Center | | Periphery | | | | |
| | | | | | | Dia. | Pitch | Dia. | Pitch | | | |
| | | | | | | | | | | | | |
| mm | mm | | mm | mm | mm | mm | mm | mm | mm | mm ² | | |
| M 2 CWG | 6.5 | 2790 | 169 | 4270±4 | 110.6 | 1.3 | 395 | 1.0 | 197.5 | 3.2776 | 3659.4 | — |
| M 2 CWH | 6.5 | 2800±2 | 169 | 4270±5 | 110.6 | 1.3 | 252 | 1.0 | 252 | 3.2769 | 3659.1 | 0.5 C |

Table 3.1 Experimental Condition (MONJU II)

| | |
|---------------------------------|------------------------------------|
| Flow Rate (m ³ /min) | 2.8~3.0 (1.4~1.5/1 assembly) |
| Sodium Temp. (°C) | 600 ±5 |
| Mass Flow Rate (kg/s) | 18.9~20.2/1 assembly |
| Oxygen Con. (PPM) | 8.5 (Claxton Eq) 23 (Eichelberger) |
| Cold Trap Min. Temp. (°C) | 143 ±1 |
| Assembly | Wire Type (M2 CWG, M2 CWH) |
| Test Loop | Sodium Flow Test Loop |

Table 4.1 Sodium Flow Test Results

| Experiment | Item | Pressure Loss Coeff. Calculation Eq. | Re Number Range | Cd Value | | Percent Increase of Pressure Loss (%) |
|-------------------------------------|----------------------|---|--|----------------------|------------------------|--|
| | | | | Re=2×10 ⁴ | Re=7.5×10 ⁴ | |
| Calculation from Water Flow Test | 0hr | $Cd=191.4 Re^{-0.1955}$ | 10 ⁴ ~ 6.6×10 ⁴ | 27.61 | 21.32 | — |
| No 1 Sodium Flow Test | 16hr (52hr) | $Cd=244.6 Re^{-0.2175}$ | 2×10 ⁴ ~ 8.8×10 ⁴ | 28.38 | 21.29 | — |
| No 2 Sodium Flow Test | 616hr (652hr) | $Cd=156.9 Re^{-0.1723}$ | 2×10 ⁴ ~ 8.6×10 ⁴ | 28.47 | 22.67 | 6.5 |
| No 3 Sodium Flow Test | 1116hr (1152hr) | $Cd=224.4 Re^{-0.2030}$ | 2.1×10 ⁴ ~ 8.5×10 ⁴ | 30.05 | 22.98 | 7.9 |
| No 4 Sodium Flow Test | 1620hr (1656hr) | $Cd=171.3 Re^{-0.1777}$ | 2.1×10 ⁴ ~ 8.4×10 ⁴ | 29.48 | 23.31 | 9.5 |
| No 5 Sodium Flow Test | 2148hr (2184hr) | $Cd=219.8 Re^{-0.1991}$ | 2.1×10 ⁴ ~ 8.4×10 ⁴ | 30.61 | 23.52 | 10.5 |
| No 6 Sodium Flow Test | (2700hr) (2736hr) | $Cd=260.6 Re^{-0.2132}$ | 2×10 ⁴ ~ 8.4×10 ⁴ | 31.55 | 23.81 | 11.8 |
| No 7 Sodium Flow Test | 3276hr (3312hr) | $Cd=211.2 Re^{-0.1946}$ | 1.9×10 ⁴ ~ 8.35×10 ⁴ | 30.75 | 23.77 | 11.7 |
| No 8 Sodium Flow Test | 3828hr (3864hr) | $Cd=216.7 Re^{-0.1987}$ | 2.3×10 ⁴ ~ 8.5×10 ⁴ | 30.32 | 23.32 | 9.5 |
| No 9 Sodium Flow Test | 4308hr (4344hr) | $Cd=208.2 Re^{-0.1944}$ | 2.7×10 ⁴ ~ 8.4×10 ⁴ | 30.36 | 23.48 | 10.3 |
| No 10 Sodium Flow Test | 4787hr (4823hr) | $Cd=238.0 Re^{-0.2057}$ | 2.3×10 ⁴ ~ 8.4×10 ⁴ | 31.04 | 23.65 | 11.1 |
| Calculation from Water Flow Test | 4790hr (4847hr) | $Cd=154.2 Re^{-0.1716}$ | 10 ⁴ ~ 7.2×10 ⁴ | 28.18 | 22.46 | 5.4 |

Table 4.2(a) Hydrodynamic Test Result (M2CWG)

| M2CWH | BEFORE SODIUM FLOW TEST | | | | AFTER SODIUM FLOW TEST | | | | Percent Increase of Pressure Loss |
|--|---|-----------------------|-------------------------|--|---|------------|--------------|--|-----------------------------------|
| Pressure Loss Coefficient Position | Experimental Equation ($8.9 \times 10^3 < Re < 6.6 \times 10^4$) | Cd Value | | Allotment Rate of Pressure Loss Re= 7.5×10^4 | Experimental Equation ($1.1 \times 10^4 < Re < 7.2 \times 10^4$) | Cd Value | | Allotment Rate of Pressure Loss Re= 7.5×10^4 | Re= 7.5×10^4 (%) |
| | | Re 2×10^4 | Re 7.5×10^4 | | | Re 2 10 | Re 7.5 10 | | |
| Total | $Cd=196.0 Re^{-0.1963}$ | 28.05 | 21.64 | — | $Cd=162.4 Re^{-0.1753}$ | 28.62 | 22.70 | — | 4.9 ± 0.6 |
| Entrance Nozzle | $Cd= 3.07 Re^{-0.0211}$ | 2.49 | 2.42 | 0.11 | $Cd= 3.01 Re^{-0.0179}$ | 2.52 | 2.46 | 0.11 | 1.7 ± 1.6 |
| Lower Section Shield | $Cd= 7.28 Re^{-0.1358}$ | 1.90 | 1.59 | 0.07 | $Cd= 5.06 Re^{-0.0996}$ | 1.89 | 1.65 | 0.07 | 3.8 ± 2.6 |
| Bundle (Calculated from friction factor) | $Cd=217.4 Re^{-0.2314}$ | 21.98 | 16.19 | 0.75 | $Cd=183.6 Re^{-0.2121}$ | 22.47 | 16.97 | 0.75 | 5.0 ± 1.0 |
| Upper Section Shield | $Cd= 2.27 Re^{-0.0364}$ | 1.58 | 1.51 | 0.07 | $Cd= 2.38 Re^{-0.035}$ | 1.68 | 1.61 | 0.07 | 6.6 ± 4.5 |

| | | | | | | | | |
|---|-------------------------|---------------------------|---------------------------|---|-------------------------|---------------------------|---------------------------|---------------|
| Friction Factor of Pin Bundle | $f=0.2622 Re^{-0.2314}$ | 2.651×10^{-2} | 1.952×10^{-2} | — | $f=0.2214 Re^{-0.2121}$ | 2.710×10^{-2} | — | 5.0 ± 1.0 |
| Entrance Nozzle Pressure Loss Coefficient | $Cd=2.93 Re^{-0.0212}$ | Re= 6.85×10^4 | Re= 2.57×10^5 | — | $Cd=2.85 Re^{-0.0176}$ | Re= 6.85×10^4 | Re= 2.57×10^5 | — |

Re; Re Number at Pin Bundle

Table 4.2(b) Hydrodynamic Test Results (M2CWH)

| M2CWH | BEFORE SODIUM FLOW TEST | | | | AFTER SODIUM FLOW TEST | | | | Percent Increase of Pressure Loss |
|--|---|-----------------------|-------------------------|---|---|-----------------------|-------------------------|---|-----------------------------------|
| Pressure Loss Coefficient Position | Experimental Equation ($1.1 \times 10^4 < Re < 6.2 \times 10^4$) | Cd Value | | Allotment Rate of Pressure Loss $Re = 7.5 \times 10^4$ | Experimental Equation ($1.3 \times 10^4 < Re < 7.1 \times 10^4$) | Cd Value | | Allotment Rate of Pressure Loss $Re = 7.5 \times 10^4$ | $Re = 7.5 \times 10^4$ (%) |
| | | Re 2×10^4 | Re 7.5×10^4 | | | Re 2×10^4 | Re 7.5×10^4 | | |
| Total | $Cd = 193.7 Re^{-0.1949}$ | 28.11 | 21.73 | — | $Cd = 149.4 Re^{-0.1662}$ | 28.81 | 23.13 | — | 6.4 ± 0.6 |
| Entrance Nozzle | $Cd = 1.82 Re^{-0.0167}$ | 1.54 | 1.51 | 0.07 | $Cd = 1.91 Re^{-0.0189}$ | 1.58 | 1.55 | 0.07 | 2.7 ± 2.5 |
| Lower Section Shield | $Cd = 8.21 Re^{-0.1071}$ | 2.84 | 2.47 | 0.11 | $Cd = 5.26 Re^{-0.0669}$ | 2.85 | 2.63 | 0.11 | 6.5 ± 1.4 |
| Bundle (Calculated from friction factor) | $Cd = 202.9 Re^{-0.2235}$ | 22.19 | 16.51 | 0.76 | $Cd = 161.0 Re^{-0.1980}$ | 22.66 | 17.45 | 0.75 | 5.7 ± 0.8 |
| Upper Section Shield | $Cd = 5.3 Re^{-0.125}$ | 1.5 | 1.3 | 0.06 | $Cd = 4.83 Re^{-0.106}$ | 1.69 | 1.47 | 0.06 | 13.1 ± 4.9 |

| | | | | | | | | | |
|---|---------------------------|----------------------------------|----------------------------------|---|---------------------------|----------------------------------|----------------------------------|---|---------------|
| Friction Factor of Pin Bundle | $f = 0.2451 Re^{-0.2235}$ | 2.680×10^{-2} | 1.994×10^{-2} | — | $f = 0.1945 Re^{-0.1980}$ | 2.737×10^{-2} | 2.107×10^{-2} | — | 5.7 ± 0.8 |
| Entrance Nozzle Pressure Loss Coefficient | $Cd = 1.71 Re^{-0.0166}$ | 1.42 $Ree = 6.87 \times 10^4$ | 1.39 $Ree = 2.58 \times 10^5$ | | $Cd = 1.81 Re^{-0.0188}$ | 1.47 $Ree = 6.87 \times 10^4$ | 1.43 $Ree = 2.58 \times 10^5$ | | |

Re; Re Number at Pin Bundle

Ree; Re Number at Entrance Nozzle orifice